Noise–induced stabilization of bumps in systems with long–range spatial coupling

Carlo R. Laing [a,*] and André Longtin [a]

[a] *Department of Physics, University of Ottawa, 150 Louis Pasteur, Ottawa ON, Canada K1N 6N5.*

Abstract

1 Introduction

There has been much recent interest in spatially localized patches of active neurons ("bumps") as models for feature selectivity in the visual system [3,4,14], the head direction system [38], and orking memory [5,12,22,44]. Both rate models [2,3,6,14,38], in hich the firing rates of cells are the variables of interest, and net orks of spiking neurons [4,5,12,22,39], in hich the cells communicate by firing voltage "spikes", have been used in the study of such structures.

Spike frequency adaptation, in hich the discharge frequency of a neuron slo ly decreases under a constant stimulus, is ubiquitous in cortical neurons [26]. One previous study of rate and spiking models capable of bump formation, [14], noted that the inclusion of adaptation caused previously neutrally stable stationary bumps to become unstable, ith bumps that travel at a constant speed being stable instead. This presumably has a deleterious effect on the systems mentioned above hich are thought to be capable of sustaining stationary bumps. The main purpose of our ork is to sho that the addition of noise to such a system can counteract the destabilizing influence of adaptation. This "restabilizing" occurs in both spiking and rate models, and is an example, similar in spirit to stochastic resonance [9,45] and noise–enhanced propagation [17,27], of a situation in hich moderate amounts of noise are necessary for a system to behave in an optimal fashion. In the neural context of interest here, noise is associated ith random synaptic firing, as ell as conductance fluctuations, both common in real neural systems [29].

To analyze the effect of the noise, e study a spatially–extended rate model that can be reduced to a set of six ordinary differential equations, and then sho that this system of ODEs undergoes a supercritical pitchfork bifurcation [11] in bump velocity as the strength of the adaptation is increased — this is the source of the destabilization of a stationary bump as a result of including adaptation. We add noise to the normal form of the associated supercritical pitchfork bifurcation, here the variable undergoing the bifurcation is velocity, and investigate the effect of this noise on the total distance traveled (the time integral of the velocity) after the bifurcation has occurred, i.e. hen the noise–free normal form has t o stable non–zero velocity values of opposite sign. We see that for lo noise values the distance traveled is proportional to time, but for larger noise values the instantaneous velocity ill change signs, leading to some cancellation in the integral, and resulting in a smaller net distance traveled, as is observed in simulations of the spatially–extended net orks.

We sho that this s itching in the noisy pitchfork bifurcation, here the velocity is a continuous variable, can be further simplified to a persistent random alk [32] in hich a particle moves at a constant speed to either the right or the left on a line, and the probability of *changing* direction is constant (and related to the noise level through an Arrhenius–type rate). Both discrete and continuous–time versions of this random alk are discussed. In the continuous–time version, the position of the

for $i = 1, \ldots, N$, here the subscript i indexes the neurons, t_j^m is the mth firing time of neuron j, defined to be the times at hich V_j crosses 1 from belo , and $\delta(\cdot)$ is the Dirac delta, used to reset the voltage to zero and increment a. The function $\alpha(t)$ is a post–synaptic current, hich e take to be $\beta e^{-\beta t}$ for $t \geq 0$ and zero other ise; I_i is the constant current applied to neuron i. The connection strength bet een neuron i and neuron j is J_{ij}. The sums over m and l extend over the entire firing history of the neurons in the net ork and the sum over j extends over the hole net ork. The variable a_i is incremented by an amount A/τ_a henever V_i reaches 1 from belo , and decays exponentially ith time constant τ_a other ise.

For $A = 0$, the system (1) is kno n to support "bumps", spatially localized patches of active neurons [22]. Since the net ork is invariant ith respect to spatial translation, there is actually a continuum of bumps, parametrized by their spatial location [14,22]. For small A, this behavior persists, but as A is increased further, a stationary bump loses stability to a traveling bump that can travel either left ards or right ards. Figure B.1 sho s the absolute value of the speed of a bump as a function of A (adaptation strength), and an example of a traveling bump is sho n in Figure B.2, left. Parameters for Figures B.1, B.2 and B.3 are $I_i = 0.95$, $N = 60$, $\tau_a = 5$, $\beta = 0.5$ and

$$J_{ij} = 5.4\sqrt{\frac{28}{\pi}} \exp\left[-28\left(\frac{i-j}{N}\right)^2\right] - 5\sqrt{\frac{20}{\pi}} \exp\left[-20\left(\frac{i-j}{N}\right)^2\right] \qquad (3)$$

i.e. neurons excite nearby neighbors but inhibit distant ones. This form of coupling is sometimes referred to as "Mexican–hat" [6], and is prevalent in many parts of the nervous system. Note that J_{ij} depends only on the difference $|i - j|$.

The reason that adaptation causes a bump to move is as follo s: adaptation can be thought of as a slo , activity–dependent subtractive current. Once a bump is moving, this subtractive current ill be greater in magnitude at the trailing edge of the bump than at the leading edge, as the neurons at the trailing edge have been firing for longer. Since bumps are "attracted" to injections of positive current [6,14] (and "repelled" by negative current), the adaptation current ill cause the bump to continue moving. A small asymmetry in initial conditions is sufficient to start the bump moving.

We add noise to the system by adding/subtracting (ith equal probability, so the mean current is unchanged) current pulses of the form $\sigma e^{-t/\tau_I}$ $(t > 0)$ to/from each I e the ne P lo to O iaroe –sut .

The absolute value of this average speed during simulations of fixed duration as a function of noise level, σ, is sho n in Figure B.3. The standard deviation of the absolute value of the average speed is also sho n. For this Figure, and other similar ones, the absolute value of the average speed is $\langle |x(t)| \rangle / t$, here $x(t)$ is the distance traveled during time t and the angled brackets indicate averages over realizations, and the standard deviation of this quantity is calculated using $\sqrt{\langle |x(t)|^2 \rangle - \langle |x(t)| \rangle^2 / t}$. We see that there are t o regimes, ith a rapid transition bet een them. For lo noise, $\sigma < 0.03$, the bump travels at a constant, large velocity, to either the right or the left, but ithout s itches in direction, an example being Figure B.2, left. For strong noise, $0.1 < \sigma$, the bump's average speed is lo , as the noise seems to disrupt the mechanism (

$$\frac{\partial u(x,t)}{\partial t} = -u($$

3.1 Gaussian white noise

First e consider adding independent Gaussian hite noise terms, $\xi_i(t)$, to each of the differential equations for the a_is, i.e. e replace (9) ith

$$\tau_a \frac{da_i}{dt} = Au_i - a_i + \xi_i(t) \tag{10}$$

here $\langle \xi_i(t) \rangle = 0$, $\langle \xi_i(t)\xi_j(s) \rangle = 2D\nu_{ij}\delta(t-s)$, and $\nu_{ij} = 0$ if $i \neq j$, and 1 if $i = j$. As ith the spiking model, the average speed of these traveling bumps can be markedly reduced by adding noise to the system, as sho n in Figure B.5, even though in this case the noise has a continuous state space, rather than being shot noise as in the spiking neuron model of Section 2.

Figure B.5 is qualitatively similar to Figure B.3, but there is a difference ith regard to the variability of bump speed at lo noise levels. For lo noise levels a traveling bump in the rate model has a ell–defined velocity, but in the full spiking model a traveling bump is the result of the collective behavior of a number of units, each of hich has its o n spiking dynamics. Even if no noise is added to the system, these dynamics contribute to fluctuations in any quantity associated ith the net ork as a hole, and lead to the relatively large fluctuations in the speed of the bump at lo noise levels in Figure B.3. These fluctuations do not appear in Figure B.5 because the rate model is derived from a net ork ith an infinite number of asynchronous neurons hose fluctuations average out. The deterministic fluctuations in bump size and shape seen in Figure B.2, left, may actually act in the same ay as the noise does in Figure B.2, right, stabilizing the bump to some extent, although obviously not to the same extent as the external noise.

3.2 Colored Noise

In this section e investigate the effect of temporal correlations in the noise process. We do this by adding independent colored noise terms, $\eta_i(t)$, to each of the differential equations for the a_i's, i.e. e replace (9) ith

$$\tau_a \frac{da_i}{dt} = Au_i - a_i + \eta_i(t) \tag{11}$$

here $\langle \eta_i(t) \rangle = 0$, $\{\langle \eta_i(t)\eta_j(s) \rangle\} = \varepsilon\nu_{ij}e^{-|t-s|/\tau}$, ν_{ij} is as in Section 3.1, and $\{\cdots\}$ indicates averaging over the initial distribution of $\eta(0)$ values, taken from a Gaussian ith mean zero and variance ε [7]. This type of noise, kno n as Ornstein–Uhlenbeck noise, also has a continuous state space.

Figure B.6, top, sho s a plot of the absolute value of the average speed as a function of noise po er, ε, for different correlation times, τ, as ell as for frozen (i.e. time

independent) noise taken from the same distribution from hich the $\eta(0)$ values are chosen. Figure B.6, bottom, sho s the standard deviation of the absolute value of the average speed, plotted separately for clarity. Note the rise and then fall of the standard deviation as noise strength is increased — this behavior is explained qualitatively in Section 5.2. The qualitative behavior (slo ing do n of the bump) does not depend on the noise correlation time, but it is clear that hen the noise level is high enough to significantly slo the bump, a larger value of τ leads to a smaller average velocity. This can be understood in terms of the limiting case, frozen noise, here the noise can "pin" the bump so that it has zero velocity for all time, ith the spatial disorder overcoming the adaptation–induced tendency to move. (See [14,22] for examples of the pinning of a bump ith spatial disorder in net orks of spiking neurons. A similar phenomenon is the failure of a calcium ave to propagate due to inhomogeneities [43].) When the noise is correlated over a significant amount of time, τ, it is possible for the bump to be pinned for an amount of time comparable to this before moving again hen the noise has significantly changed. These "pinning episodes" contribute to the lo er average velocity. Thus, externally imposed (and slo ly varying) disorder may be more effective in slo ing the bump than fast intrinsic noise.

This behavior is further illustrated in Figure B.7, here e sho the absolute value of the average speed (top) and average of the absolute value of the instantaneous speed (bottom) as functions of correlation time, τ, for a noise intensity sufficient to significantly slo the bump. It is clear that for both measures of speed, bump speed decreases as the noise correlation time increases. The absolute value of the average speed is a measure of ho far the bump is from its starting position after a fixed amount of time, and is perhaps the most relevant quantity in a model of orking memory (here bump position encodes some feature of the memory), but measuring the average of the absolute value of the instantaneous speed gives a better indication of the fraction of time that a bump is "pinned" during a particular simulation.

Adding spatial correlations to the noise, as in e.g. [37], may change the effect of noise on the bump, but e do not investigate that here.

4 Reduction to ODEs

Having satisfied ourselves that the rate model in Section 3 behaves qualitatively the same as the full spiking model in Section 2, both ith and ithout noise, e ill no sho that the bifurcation from stationary to traveling bumps in (6)-(7) is a pitchfork bifurcation [11]. By an appropriate choice of the function J in (6), e can reduce the system (6)-(7) to a set of six ordinary differential equations. Consider the system (6)-(7), here $\Omega = [0, 2\pi)$ ith periodic boundary conditions and $J(v) = B + C\cos v$, so that $J(x-y) = B + C\cos x\cos y + C\sin x\sin y$. (If C is positive, this choice of J can be thought of as the first t o terms in a Fourier series expansion of a "Mexican–hat" type J [3,14].) We can expand u and a as Fourier series in x, but by doing so

$$g(\alpha-\gamma,R,\theta,\kappa,\psi)$$
$$=\int_0^{2\pi} F[I+\alpha-\gamma+R\cos(y-\theta)-\kappa\cos(y-\theta-\psi)]\cos y\,dy \tag{21}$$

$$h(\alpha-\gamma,R,\theta,\kappa,\psi)$$
$$=\int_0^{2\pi} F[I+\alpha-\gamma+R\cos(y-\theta)-\kappa\cos(y-\theta-\psi)]\sin y\,dy \tag{22}$$

Note that f, being proportional to the spatial average of the bump's activity, does not depend on θ, the position of the center of the bump. We assume that R and κ are never zero, as such a solution ould not correspond to a bump. Apart from transients, equations (14)-(19) are equivalent to equations (6)-(7), and e no sho that stationary and moving bumps are solutions of (14)-(19), and that the transition

particular, $b_1 = 0$, making the right hand side of (16) zero, as it must be for a fixed point. Thus (14)-(19) has a continuum of fixed points, parametrized by the position of the maximum of the bump.

4.2 Moving bumps

From simulations of the rate model (6)-(7), e expect a fixed point of (14)-(19) to become unstable as A is increased, and the system to have an attractor on hich $\theta(t) = \omega t$ for some non–zero and constant ω, ith all other variables constant. Since $\theta \in \mathbf{S}^1$, this attractor is actually a periodic orbit. Assuming that e are on the attractor, $d\theta/dt = \omega$ and (18) and (19) give us

$$\psi = -\tan^{-1}(\tau\omega) \tag{26}$$

so that ψ is nonzero if and only if ω is nonzero. Also, remembering that $-\pi/2 < \psi < \pi/2$ for a stable bump, e see that ψ and ω have opposite signs. This is in agreement ith our intuition about the model, viz. that the activity in a lags behind the activity in u. Equations (17) and (18) give $\gamma = A\alpha$ and $\kappa = AR\cos\psi < AR$, so the peak height in a of a moving bump is less than that of a stationary one. Substituting these values for ψ, κ and γ into (14)-(15) e see that on the attractor, α and R must simultaneously solve

$$\alpha = Bf\left[(1-A)\alpha, R, AR\cos\{-\tan^{-1}(\tau\omega)\}, -\tan^{-1}(\tau\omega)\right] \tag{27}$$

and

$$\begin{aligned} R = C\Big\{&\cos(\omega t)g\left[(1-A)\alpha, R, \omega t, AR\cos\{-\tan^{-1}(\tau\omega)\}, -\tan^{-1}(\tau\omega)\right] \\ &+ \sin(\omega t)h\left[(1-A)\alpha, R, \omega t, AR\cos\{-\tan^{-1}(\tau\omega)\}, -\tan^{-1}(\tau\omega)\right]\Big\} \end{aligned} \tag{28}$$

here the value of t in (28) is irrelevant, since

i.e. a scalar equation in one variable, parametrized by A. We rite it in this form because e kno that $\omega = 0$ is al ays a fixed point of (14)-(19), and, from section 4.1, there is no dependence on t in (29). ($\omega = 0$ is al ays a solution of (30) because if $\omega = 0$, $\psi = 0$, and therefore b_1 in the Fourier representation of $F[\cdot]$, (23), is zero, making the right hand side of (16) zero.) We also kno that $\omega G(\omega, A)$ is an odd function of ω (therefore $G(\omega, A)$ is even in ω). To see this, note that $\tilde{R}(-\omega, A) = \tilde{R}(\omega, A)$, and it can be sho n that $g(\alpha - \gamma, R, -\omega t, \kappa, -\psi) = g(\alpha - \gamma, R, \omega t, \kappa, \psi)$ and $h(\alpha - \gamma, R, -\omega t, \kappa, -\psi) = -h(\alpha - \gamma, R, \omega t, \kappa, \psi)$, so the left hand side of (29) is an odd function of ω.

We expect t o nonzero solutions of (30), of equal magnitude but opposite sign, to be created as A increases through some critical value. To sho that this occurs, e expand $G(\omega, A)$ as a Taylor series. We can expand about $\omega = 0$, but should not expand about $A = 0$, as this is a singular limit. Instead, e choose to expand about $A = 0.15$, i.e. e rite

$$G(\omega, A) = \mu_1 + \mu_2(A - 0.15) + \mu_3\omega^2 + \mu_4(A - 0.15)^2 + \cdots \tag{31}$$

The value $A = 0.15$ as chosen arbitrarily — e expect the bifurcation to occur at a small positive value of A. The series expansion, (31), ill be more accurate for values of A closer to the bifurcation value ($A \approx 0.165$, from Figure B.8) for a given truncation of the series, but as can be seen belo , this value orks ell. Approximate values of the four coefficients $\mu_1, \ldots, \mu_4$ can be found by numerically differentiating (30), as explained in [25]. For the parameter values given in Section 3 e find $\mu_1 \approx -0.0438$, $\mu_2 \approx 2.6012$, $\mu_3 \approx -9.986$ and $\mu_4 \approx 1.762$. In Figure B.8 e have plotted ith a solid line

$$\omega = \sqrt{\frac{-[\mu_1 + \mu_2(A - 0.15) + \mu_4(A - 0.15)^2]}{\mu_3}} \tag{32}$$

hen the expression under the square root is positive, i.e. approximate nonzero roots of (30), together ith measured values of ω for the system (6)-(7) and (14)-(19). The agreement is very good, even having truncated $G(\omega, A)$ after quadratic order.

Thus e have sho n that the instability to traveling bumps as A is increased in the integro–differential system (6)-(7) is due to a pitchfork bifurcation in the speed of a bump. The pitchfork bifurcation is supercritical.

4.3 Noisy pitchfork bifurcation

We no consider the effect of adding noise to the normal form of a supercritical pitchfork bifurcation in hich the variable is speed. Instead of examining the behavior of this variable, e look at its integral over a fixed amount of time. We can use this to derive a quantity equivalent to the absolute value of the average speed of a bump, as plotted in Figures B.3 and B.5. The intuition behind this procedure is that the velocity reverses sign at random times, and since the velocity undergoes a pitchfork

bifurcation, e make the ansatz that the main effect of noise on the hole system ill also appear in the normal form of that bifurcation [19].

Consider the system

$$\begin{aligned} \dot{\omega} &= \omega(\lambda - \omega^2) + \xi(t) \\ \dot{\theta} &= \omega \end{aligned} \tag{33}$$

here θ represents the position of the maximum of the bump and λ plays the role of A above. ξ is a Gaussian hite noise term ith autocorrelation $\langle \xi(t)\xi(s)\rangle = 2D\delta(t-s)$. $\lambda < 0$ corresponds to the case A less than the bifurcation value (~ 0.165 in Figure B.8). In this case, $\omega = 0$ is a stable fixed point, and the average velocity is zero. For $\lambda > 0$ and $D = 0$, there are t o stable values of ω, namely $\pm\sqrt{\lambda}$, corresponding to left and right ard–moving bumps. The absolute value of the velocity is then $\sqrt{\lambda}$ hen $\lambda > 0$ and the absolute value of the distance moved after time t, i.e.

$$|\theta(t) - \theta($$

5 Persistent Ra

and

$$r_{n+1}(x) = pr_n(x+1) + (1-p)q_n(x+1) \tag{40}$$

$P(x)$ for a given n is the sum of $r_n(x)$ and $q_n(x)$. N

The continuous time version of a persistent random walk is the stochastic differential equation

$$\frac{dx}{dt} = I(t) \tag{47}$$

where $I(t) \in \{-v, v\}$ and the probability that $I(t)$ switches from $-v$ to v, or from v to $-v$, in time interval dt is $\frac{1}{2}\beta\, dt$. In other words, the velocity is just dichotomous Markovian noise. Then the probability density function of x, $p(x,t)$, is known [13,16,41] to satisfy the integro–differential equation

$$\frac{\partial p(x,t)}{\partial t} = v^2 \int_{-\infty}^{t} e^{-\beta(t-s)} \frac{\partial^2 p(x,s)}{\partial x^2}\, ds \tag{48}$$

t

$$\langle |x(t)| \rangle = 2\int_0^\infty xp(x,t)\,dx = e^{-\beta t/2}\left\{ vt + \frac{\beta}{2v}\int_0^{vt} xI_0\left(\frac{\beta}{2v}\sqrt{v^2t^2-x^2}\right)dx \right.$$
$$\left. + \frac{\beta t}{2}\int_0^{vt} \frac{x}{\sqrt{v^2t^2-x^2}} I_1\left(\frac{\beta}{2v}\sqrt{v^2t^2-x^2}\right)dx \right\}$$
$$= vte^{-\beta t/2}\left\{ I_1\left(\frac{\beta t}{2}\right) + I_0\left(\frac{\beta t}{2}\right)\right\} \tag{51}$$

here the angled brackets represent averaging over realizations.

To obtain the second moment of $|x(t)|$ (or $x(t)$) e note that after taking the spatial Fourier transform of $p(x,t)$,

$$\sigma(s,t) \equiv \int_{-\infty}^{\infty} p(x,t)e^{-isx}\,dx \tag{52}$$

e have

$$\langle |x(t)|^2 \rangle = \langle x^2(t) \rangle = -\left.\frac{\partial^2 \sigma(s,t)}{\partial s^2}\right|_{s=0} \tag{53}$$

As derived in Appendix A, eq. (A.5),

$$\sigma(s,t) = e^{-\beta t/2}\left(\beta\right.$$

Another way to calculate the second moment is to note that the autocorrelation of $I(t)$ is [13,16,36]

$$\langle I(s)I(r)\rangle = v^2 e^{-\beta|s-r|} \tag{58}$$

so that

$$\langle x^2(t)\rangle = \left\langle \int_0^t I(s)\,ds \int_0^t I(r)\,dr \right\rangle = \int_0^t \int_0^t \langle I(s)I(r)\rangle\,ds\,dr = \frac{2v^2(\beta t - 1 + e^{-\beta t})}{\beta^2} \tag{59}$$

Alternatively [32], by multiplying (49) by x^2 and then integrating over x, one obtains the differential equation satisfied by the second moment

$$\frac{d^2\langle x^2\rangle}{dt^2} + \beta\frac{d\langle x^2\rangle}{dt} = 2v^2 \tag{60}$$

The appropriate initial conditions are $\langle x^2\rangle(0) = 0$, $d\langle x^2\rangle/dt|_{t=0} = 0$, and with these, (60) hat

of this noisy normal form. (Bump destabilization is also seen if synaptic depression — another important feature of single neurons — is included, rather than spike frequency adaptation, and adding noise to the depression dynamics can restabilize the bump.)

As a further simplification, e modeled the noisy pitchfork bifurcation as a persistent random alk, in hich a particle moves at a constant speed, but the probability of changing direction is constant (and related to noise level through an Arrhenius–type rate). If this process is taken to be continuous in time, the probability density function for position obeys the telegrapher's equation, hich has an explicit solution. From this solution e can explicitly construct the mean and standard deviation of the absolute value of the average speed of the particle (quantities that are easily measured from simulations of a full net ork, the particle being the bump in this case) and they agree quantitatively ith the behavior of the full net ork model.

One aspect of the behavior of a spatially–extended system is not ell captured by a persistent random alk: for high noise levels, the position of the maximum of a bump does not necessarily move continuously. The form of the coupling, (3), promotes local activity hile suppressing more distant activity, and at high noise levels there can be ongoing "competition" bet een bumps in a form of " inner takes all" contest. Since the domain is spatially extended, a bump may appear some distance from one that is in the process of disappearing, leading to an effective "jump" in the position of the currently highest bump. (This type of behavior as also seen in [14], in response to a suddenly–moved stimulus.) For both the noisy normal form (33) and the persistent random alks in Section 5, the particle is assumed to move continuously, so this type of jumping ill not be captured by these simplified models.

"Restabilization by noise" of a spatiotemporal pattern does not seem to have been discussed else here, although several papers [8,20] contain results regarding the effects of noise strength (manipulated indirectly by changing the number of Bro nian alkers in a simulation) on moving "spots" in simulations of excitable media. Our results are an example in the same spirit as stochastic resonance, in hich moderate amounts of noise act in a beneficial ay (at least in the context of orking memory, here a moving bump ould be seen to have a detrimental effect on the task). It is not clear hich aspects of these systems that support bumps (spatially–extended coupling, a slo variable, traveling structures that appear through a pitchfork bifurcation in speed) are necessary for this restabilization, and the question of hich other systems [6,33] sho such behavior is an interesting and open one. Figure B.4 sho s a counter–example of noise–induced restabilization, here noise causes a traveling ave to break up, rather than slo do n.

We have also studied both integrate–and–fire and rate models incorporating synaptic depression [1] rather than, or in addition to, spike frequency adaptation, and such net- orks also sho destabilization of stationary bumps as the strength of the depression is increased and restabilization hen noise is added to the dynamics of the depression. This ill be reported else here [24]. Models of t o–species reaction–diffusion systems

ith global coupling [18,21] have been observed to support stationary "spots" and "standing pulses", hich begin to move as a parameter is varied, and a similar phenomenon has been seen in both a model three–component reaction–diffusion system in hich the only coupling is by diffusion [35], and a pair of coupled Ginzburg–Landau equations [40]. The effects of noise on such systems remains to be investigated.

Acknowledgements

We thank Brent Doiron for a critical reading of the manuscript. This ork as supported by NSERC and a PREA a ard from the government of Ontario.

A Solution of the telegrapher's equation

Since the derivation of the solution of this equation in [32] is incorrect, and that in [15] has a number of typographical errors, e rederive the solution here, follo ing [15]. The telegrapher's equation is

$$\frac{\partial^2 p}{\partial t^2} + \beta \frac{\partial p}{\partial t} = v^2 \frac{\partial^2 p}{\partial x^2} \tag{A.1}$$

ith initial conditions $p(x,0) = \delta(x)$ and $\partial p(x,t)/\partial t|_{t=0} = 0$. The Fourier transform of p is

$$\sigma(s,t) = \int_{-\infty}^{\infty} p(x,t) e^{-isx}\, dx \tag{A.2}$$

hich satisfies

$$\frac{d^2\sigma}{dt^2} + \beta \frac{d\sigma}{dt} + v^2 s^2 \sigma = 0 \tag{A.3}$$

ith initial conditions $\sigma(s,0) = 1$ and $d\sigma(s,t)/dt|_{t=0} = 0$. The solution of (A.3) ith these initial conditions is

$$\begin{aligned}\sigma(s,t) &= e^{-\beta t/2}\left[\cos\left(t\sqrt{v^2 s^2 - \beta^2/4}\right)\right. \\ &\quad \left. + \frac{\beta}{2\sqrt{v^2 s^2 - \beta^2/4}} \sin\left(t\sqrt{v^2 s^2 - \beta^2/4}\right)\right] \qquad \text{(A.4)} \\ &= e^{-\beta t/2}\left(\frac{\beta}{2} + \frac{\partial}{\partial t}\right)\left\{\frac{1}{\sqrt{v^2 s^2 - \beta^2/4}} \sin\left(t\sqrt{v^2 s^2 - \beta^2/4}\right)\right\} \qquad \text{(A.5)}\end{aligned}$$

Since p is real, the inverse Fourier transform of (A.5) is

$$p(x,t) = \frac{e^{-\beta t/2}}{2\pi}\left(\frac{\beta}{2}+\frac{\partial}{\partial t}\right)\int_{-\infty}^{\infty}\frac{\cos(sx)}{\sqrt{v^2s^2-\beta^2/4}}\sin\left(t\sqrt{v^2s^2-\beta^2/4}\right)ds \tag{A.6}$$

$$= \frac{e^{-\beta t/2}}{2v}\left(\frac{\beta}{2}+\frac{\partial}{\partial t}\right)\left\{H(vt-|x|)I_0\left(\frac{\beta}{2v}\sqrt{v^2t^2-x^2}\right)\right\} \tag{A.7}$$

and performing the differentiation gives (50).

References

[1] L. F. Abbott, J. A. Varela, K. Sen and S. B. Nelson. Synaptic depression and cortical gain control. Science. **275** (1997), 220-223.

[2] .

$\hbar$F

[13] P. Hänggi and P. Riseborough. Activation rates in bistable systems in the presence of correlated noise. Phys. Rev. A **27**, (1983). 3379-3382.

[14] D. Hansel and H. Sompolinsky. Modeling feature selectivity in local cortical circuits. In Methods in Neuronal Modeling: From Ions to Networks. Ed. C. Koch and I. Segev. MIT Press (1998). 499-567.

[15] P. Chr. Hemmer. On a generalization of Smoluchowski's diffusion equation. Physica **27** (1961), 79-82.

[16] W. Horsthemke and R. Lefever. Noise–induced Transitions. Series in Synergetics, Vol. 15. Springer–Verlag, 1984.

[17] P. Jung, A. Cornell–Bell, F. Moss, S. Kadar, J. Wang and K. Showalter. Noise sustained waves in subexcitable media: From chemical waves to brain waves. Chaos **8**(3) (1998), 567-575.

[18] S. Kawaguchi and M. Mimura. Collision of travelling waves in a reaction diffusion system with global coupling effect. SIAM J. Appl. Math. **59**(3), (1999), 920-941.

[19] E. Knobloch and K. A. Wiesenfeld. Bifurcations in fluctuating systems: the center–manifold approach. J. Stat. Phys. **33**(3), (1983), 611-637.

[20] M. Kostur and L. Schimansky–Geier. Simulations of localized dissipative structures in excitable media by an ensemble of Brownian walkers. Acta Phys. Polon. B **32**(2), (2001), 351-360.

[21] K. Krischer and A. Mikhailov. Bifurcation to traveling spots in reaction–diffusion systems. Phys. Rev. Lett. **73**(23), (1994), 3165-3168.

[22] C. R. Laing and C. C. Chow. Stationary bumps in networks of spiking neurons. Neural Comp. **13** (7), (2001), 1473-1494.

[23] C. R. Laing and A. Longtin. Stabilization of spatiotemporal patterns by noise. Submitted to Phys. Rev. Lett. (2001).

[24] C. R. Laing and A. Longtin. In preparation, 2001.

[25] C. R. Laing, A. McRobie and J. M. T. Thompson, The post–processed Galerkin method applied to non–linear shell vibrations. Dyn. Stab. Systems **14** (1999), 163-181.

[26] Y.-H. Liu and X.-J. Wang. Spike–frequency adaptation of a generalized leaky integrate–and–fire model neuron. J. Comp. Neurosci. **10** (2001), 25-45.

[27] M. Löcher, N. Chatterjee, F. Marchesoni, W. L. Ditto and E. R. Hunt. Noise sustained propagation: local versus global noise. Phys. Rev. E. **61**(5), (2000), 4954-4961.

[28] A. Longtin. Noise–induced transitions at a Hopf bifurcation in a first–order delay–differential equation. Phys. Rev. A **44**(8) (1991), 4801-4813.

[29] A. Manwani and C. Koch. Detecting and estimating signals in noisy cable structures, I: neuronal noise sources. Neural Comp. **11**(8) 1999, 1797-1829.

[30] J. Masoliver, K. Lindenberg and B. J. West. First–passage times for non–Markovian processes. Phys. Rev. A **33**, (1986), 2177-2180.

B Figures

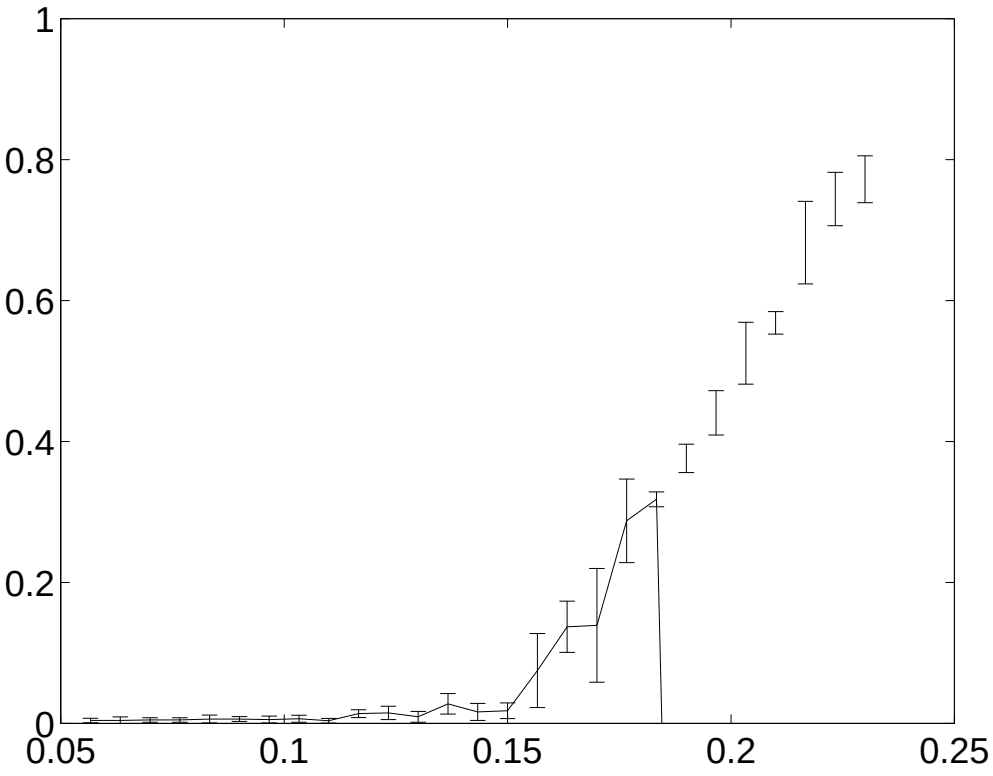

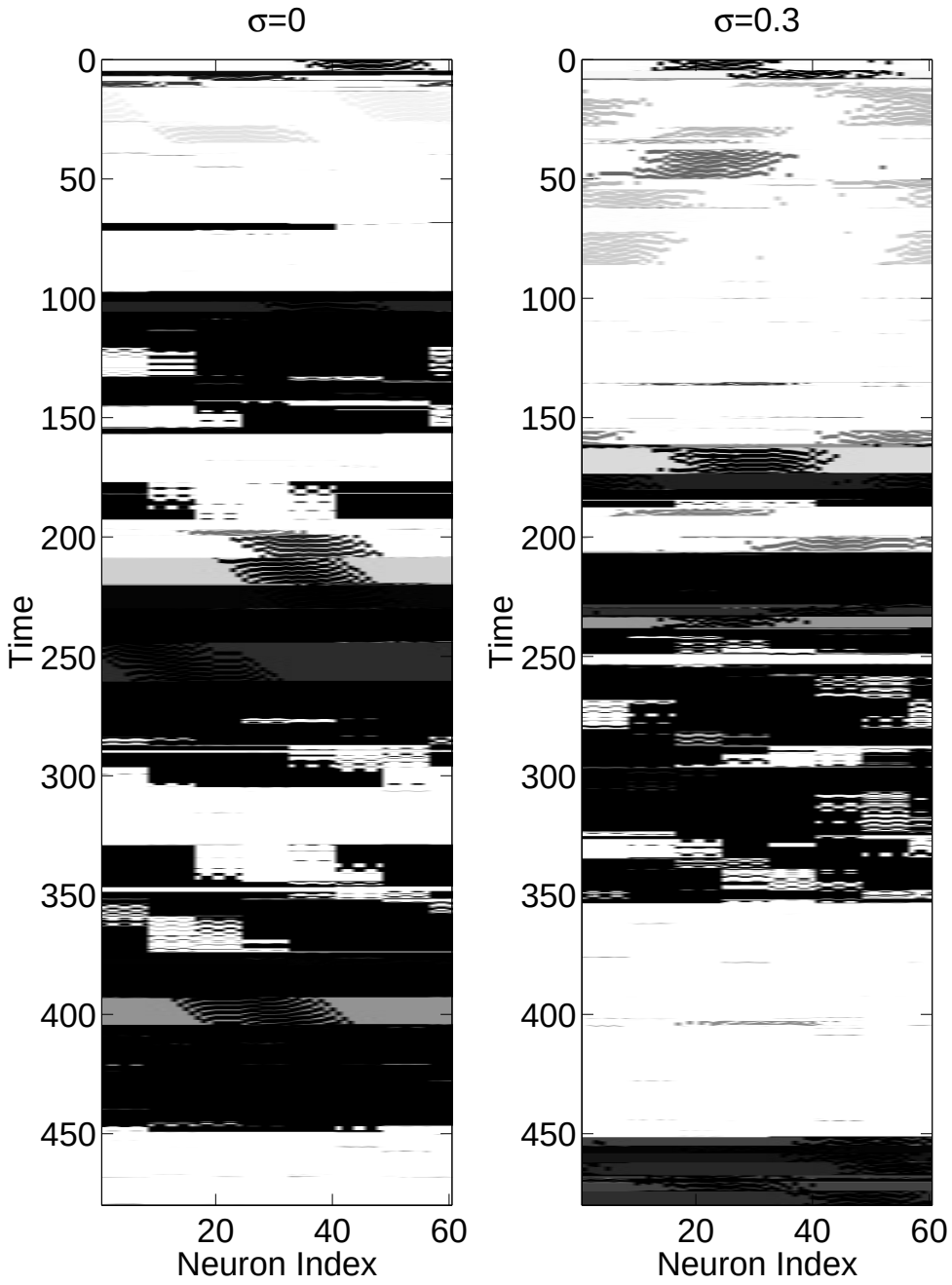

Fig. B.2. Rastergrams of the activity in the integrate–and–fire network (1)-(2). Left panel: $\sigma = 0$ (i.e. no noise), right panel: $\sigma = 0.3$. $A = 0.2$ for both. A "dot" represents the firing of an individual neuron. The sloped bands represent moving localized bumps of activity (recall that the boundary conditions are periodic). The fluctuations in bump size and shape in the left panel are of deterministic origin — see text for discussion.

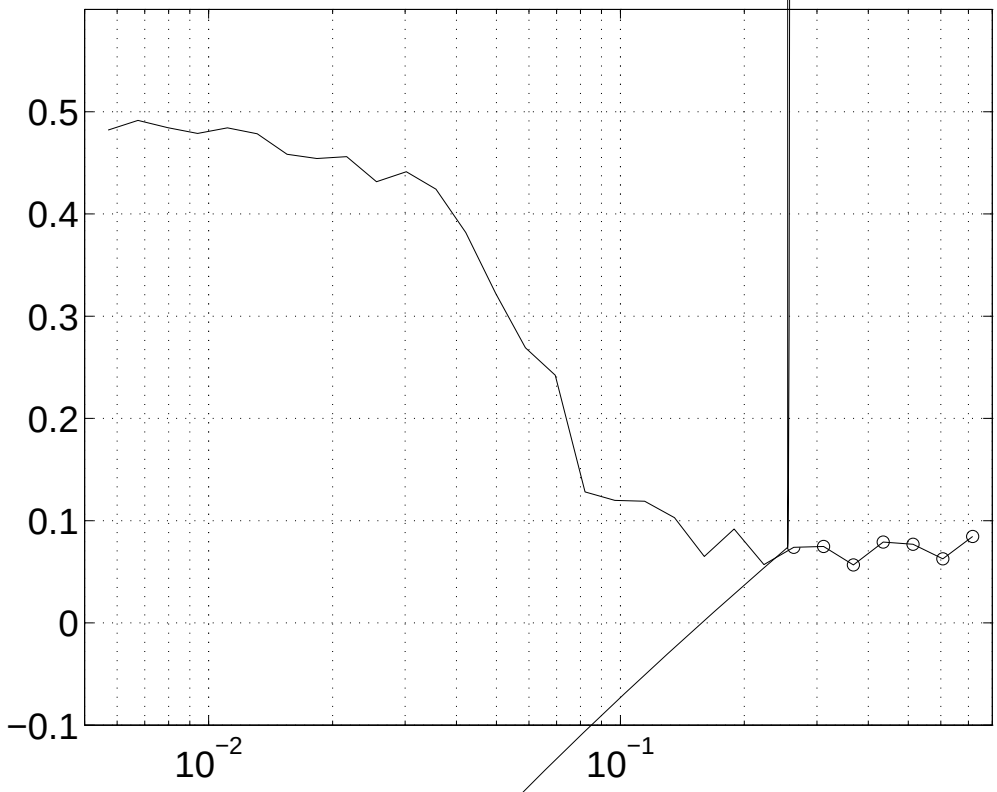
0.5
0.4
0.3
0.2
0.1
0
−0.1
10^{-2}
10^{-1}

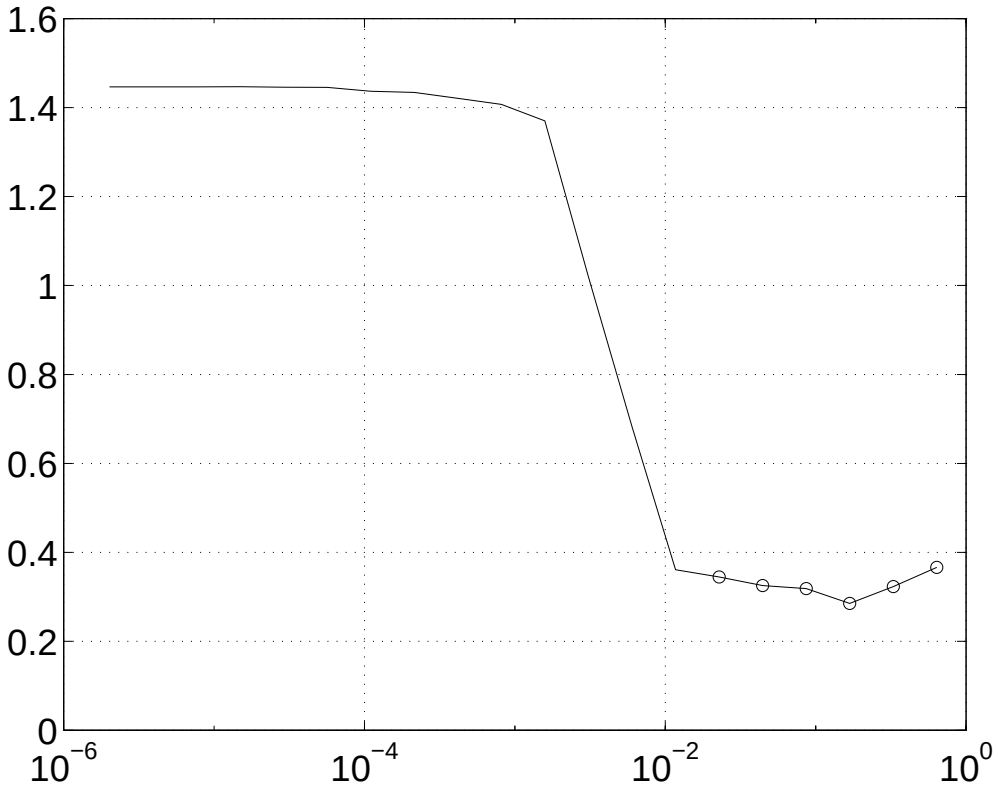
1.6
1.4
1.2
1
0.8
0.6
0.4
0.2
0
10^{-6}
10^{-4}
10^{-2}
10^{0}

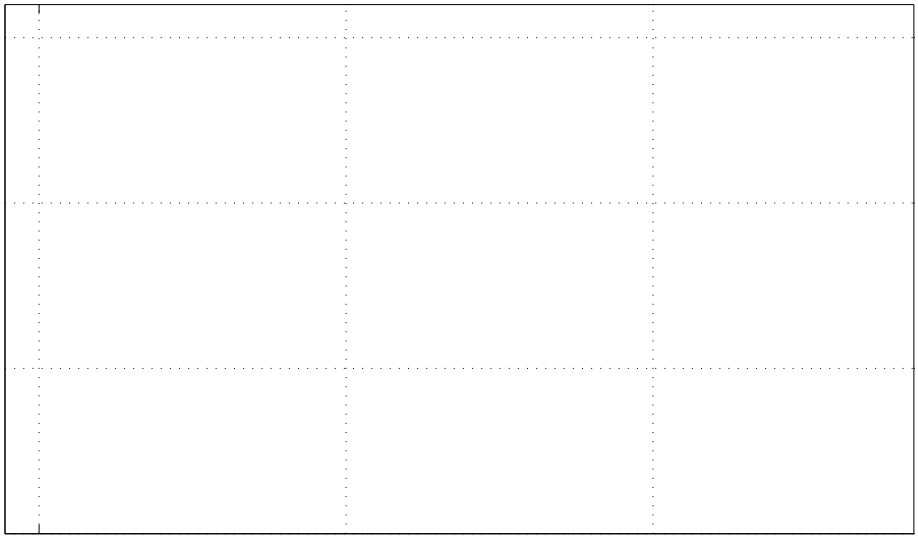

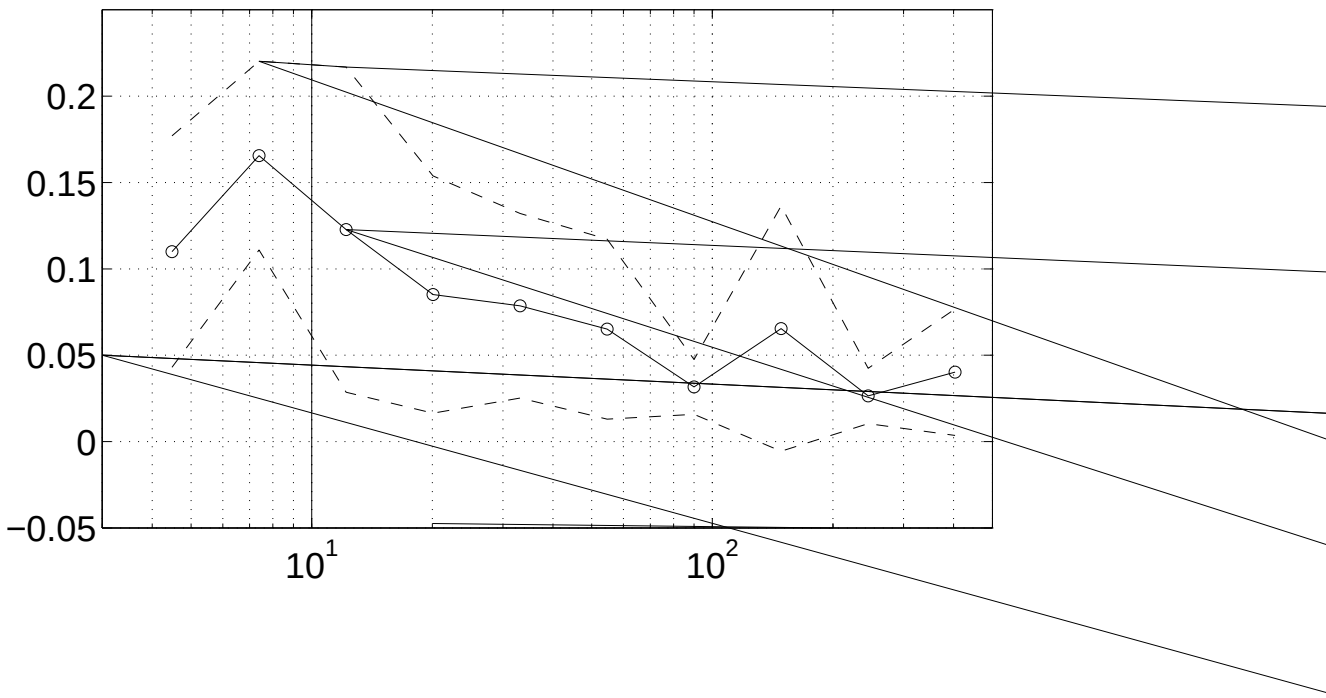
0.2
0.15
0.1
0.05
0
−0.05
10^1
10^2

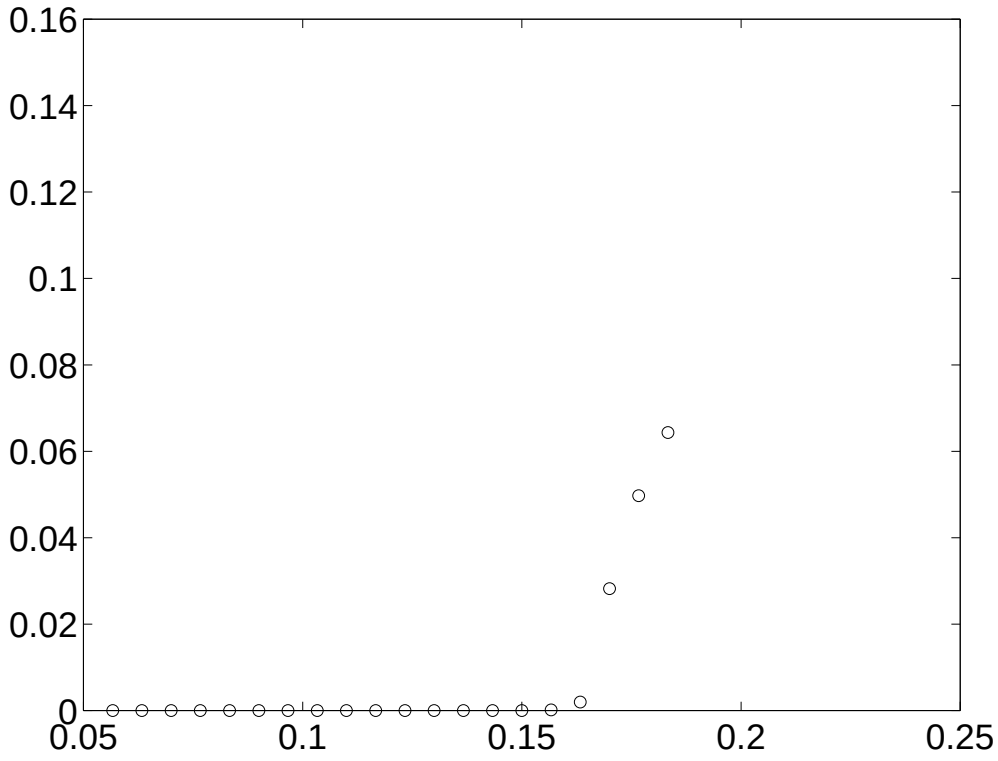
0.16
0.14
0.12
0.1
0.08
0.06
0.04
0.02
0
0.05
0.1
0.15
0.2
0.25

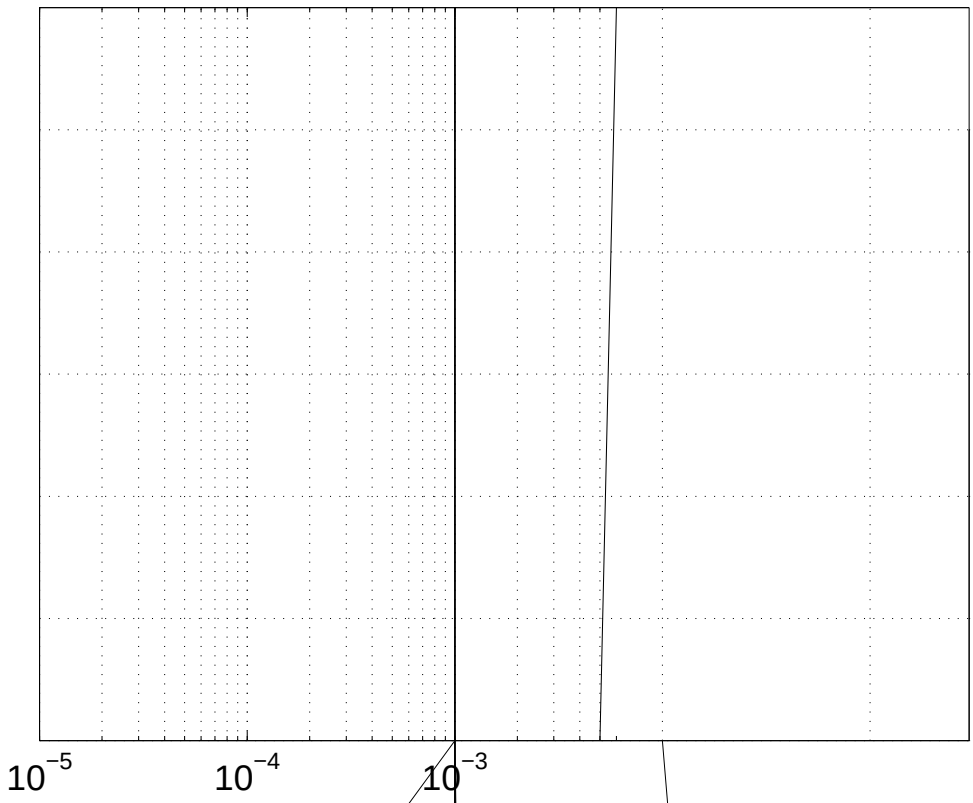
10^{-5}
10^{-4}
10^{-3}

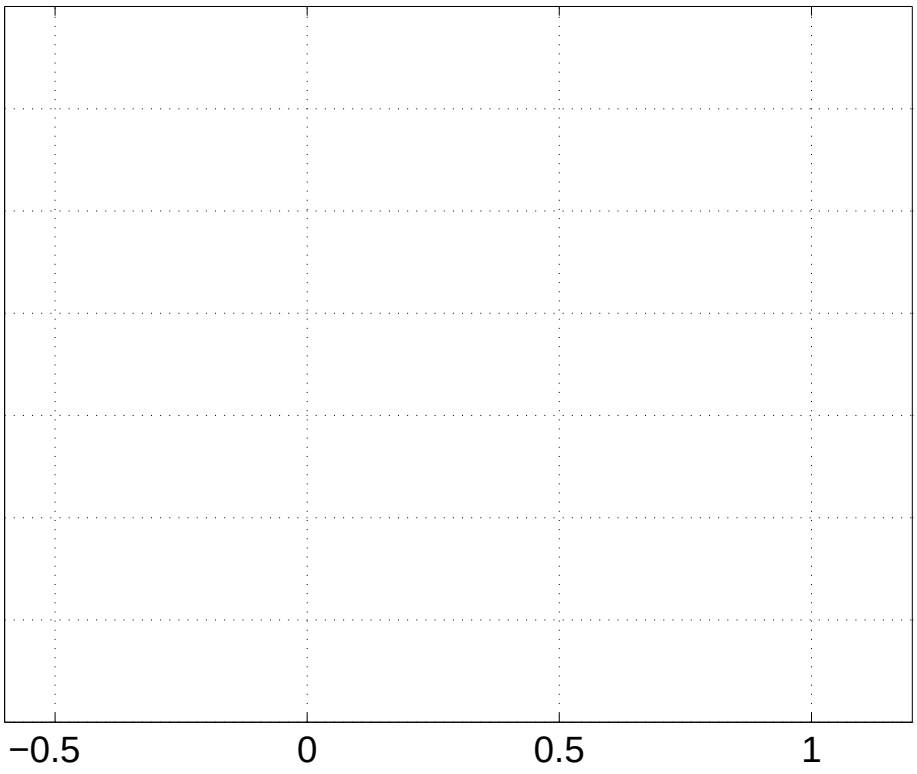
−0.5
0
0.5
1

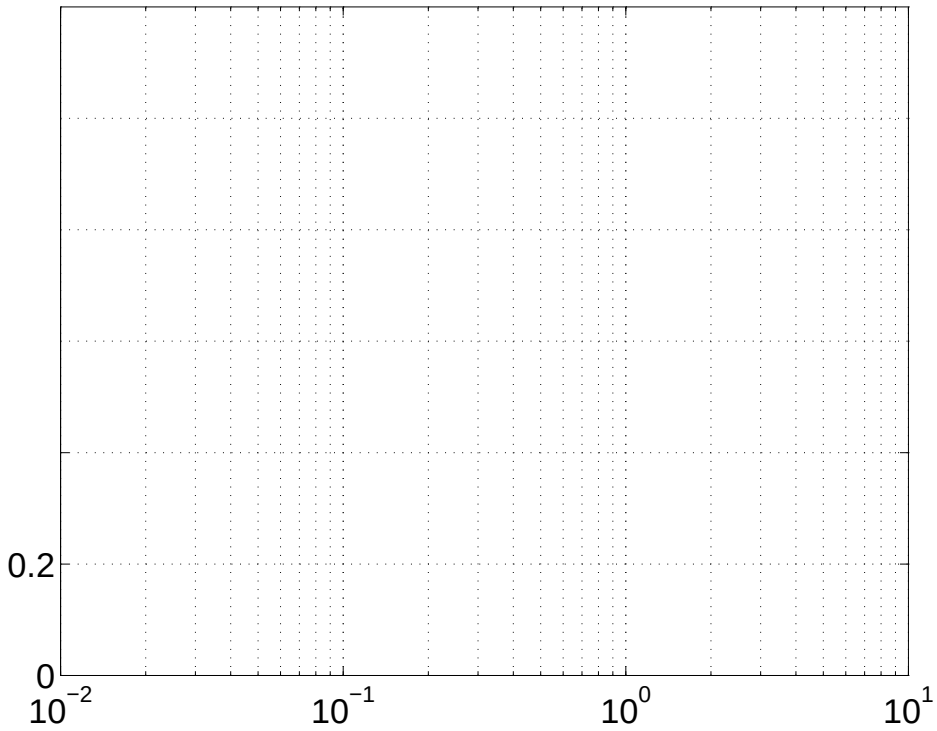
0.2
0
10^{-2}
10^{-1}
10^{0}
10^{1}

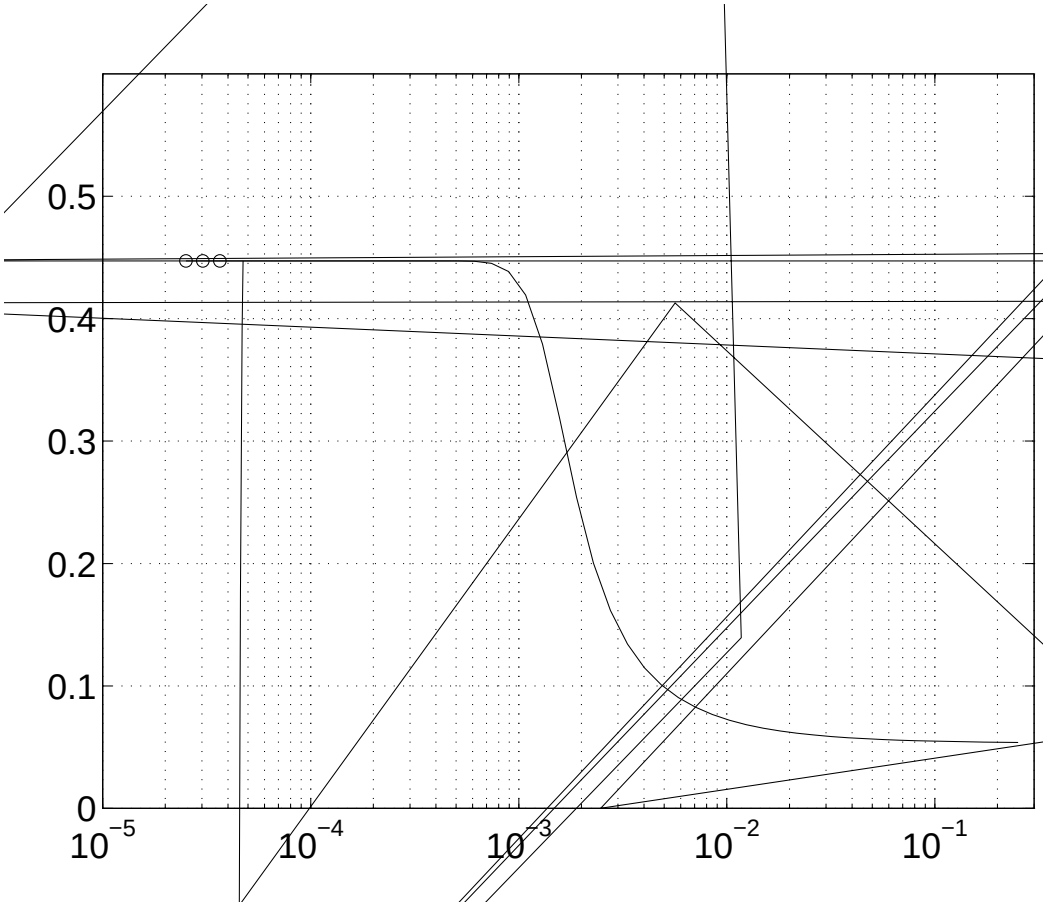
0.5
0.4
0.3
0.2
0.1
0
10^{-5}
10^{-4}
10^{-3}
10^{-2}
10^{-1}

C Tables

Path	Probability	Distance
000		